Rapid Fabrication of Micro- and Nanoscale Patterns by Replica Molding from Diatom Biosilica

ARTICLE *in* ADVANCED FUNCTIONAL MATERIALS · AUGUST 2007

Impact Factor: 11.81 · DOI: 10.1002/adfm.200600872

ADVANCED FUNCTIONAL MATERIALS

FULL PAPER

DOI: 10.1002/adfm.200600872

Rapid Fabrication of Micro- and Nanoscale Patterns by Replica Molding from Diatom Biosilica**

By *Dusan Losic*,* *James G. Mitchell*, *Ratnesh Lal*, and *Nicolas H. Voelcker**

Diatoms are single-celled micro-algae that possess an exoskeleton (called frustule) comprised of diverse and highly ordered 3D porous silica structures and that hold considerable promise for biological or biomimetic fabrication of nanostructured materials and devices. We have used, for the first time, a soft lithographic approach of replica molding to replicate porous diatom structures into polymers. Two centric diatom species, *Coscinodiscus sp.*, *Thalassiosira eccentrica* cultured in our laboratory were used as masters for replication. In the first step, replica molding onto soft and elastic polymer using poly(dimethylsiloxane) PDMS produced a negative replica of the diatom frustule. These PDMS replicas were then used as a mold to fabricate the positive polymer replicas of diatoms using a mercaptol ester type UV curable polymer (NOA 60). Fabricated polymer replicas were characterized using scanning electron microscopy (SEM) and atomic force microscopy (AFM). In all cases, diatom micro- and nanoscale porous structures were successfully transferred with high precision into polymer replicas. Such an accomplishment effectively demonstrates the potential for using diatoms as blueprints for rapid and simple fabrication of polymer nanostructures. The prepared replicas were used as diffraction gratings and as nanowells to hold polymeric nanoparticles effectively demonstrating the functional properties of these biomimetic structures.

1. Introduction

Patterned structures or surfaces are of considerable importance in many areas of modern science and technology such as microelectronics, information storage, material science, chemistry, biotechnology and microfluidics.[1] A wide range of fabrication techniques have been developed in the microelectronics industry including deep and extreme UV photolithography, phase shift photolithography, electron beam writing, focused ion beam lithography and x-ray lithography.[2] These techniques though elegant are costly in capital and operating costs, thus making them inaccessible to many potential users. Alternative simple and cost-effective techniques such as imprint lithography, soft lithography, capillary force lithography and polymer transfer printing have been developed to broaden accessibility and diversify capability.[2–5] In particular, soft lithography, which is based on a soft polymer mold such as poly(dimethylsiloxane) (PDMS) has been widely adopted for transferring patterns onto various surfaces (microcontact printing) and easy replication of complex nanostructures (replica molding).[6,7] The application of these low cost fabrication techniques has been demonstrated in manufacturing of integrated circuits, microfluidic devices, optical devices and biosensors.[8]

Biological materials and processes are a relatively new source of inspiration for the design and fabrication of nanostructured materials.[9] Many organisms synthesize inorganic structures into intricate architectures with ordered micro-to-nanoscale features that cannot typically be replicated through laboratory synthesis. A wide range of materials (metallic, inorganic or polymeric) with nanostructured geometries (particles, wires, tubes or pores) have been synthesized using biomaterials or bioinspired processes.[9c,10] The amorphous silica exoskeletons (frustules) of the single-celled algae called diatoms are one of the most spectacular examples of biologically evolved nanostructured materials.[11] Each of the estimated 10^5 diatom species has a specific frustule shape decorated with a unique pattern of nano-sized features such as pores, ridges, spikes and spines.[11] Each frustule in addition often features several hierarchical layers of porous membranes differing in feature size and pattern. A variety of potential applications for diatom frustules, including optics, photonics, catalysis, biosensing, drug delivery, filtration, bioencapsulations and immunoisolations have been proposed.[12] A glimpse of the remarkable diversity of pore architectures can be gained from Figure 1, which only includes images obtained from the frustule surface of three different diatoms. This variety of ordered porous structures irrefutably demonstrates precision and brilliance of natural design at the micro- and nanoscale. These patterned porous structures

[*] Dr. D. Losic, Prof. N. H. Voelcker
School of Chemistry, Physics and Earth Sciences, Flinders University
Bedford Park, Adelaide 5001, SA (Australia)
E-mail: dusan.losic@flinders.edu.au; nico.voelcker@flinders.edu.au
Dr. D. Losic, J. G. Mitchell
School of Biological Sciences, Flinders University
Bedford Park, Adelaide 5001, SA (Australia)
R. Lal
Center for Nanomedicine, University of Chicago
Chicago, IL 60637 (USA)

[**] The authors acknowledge support from Flinders University and the Australian Research Council (ARC).

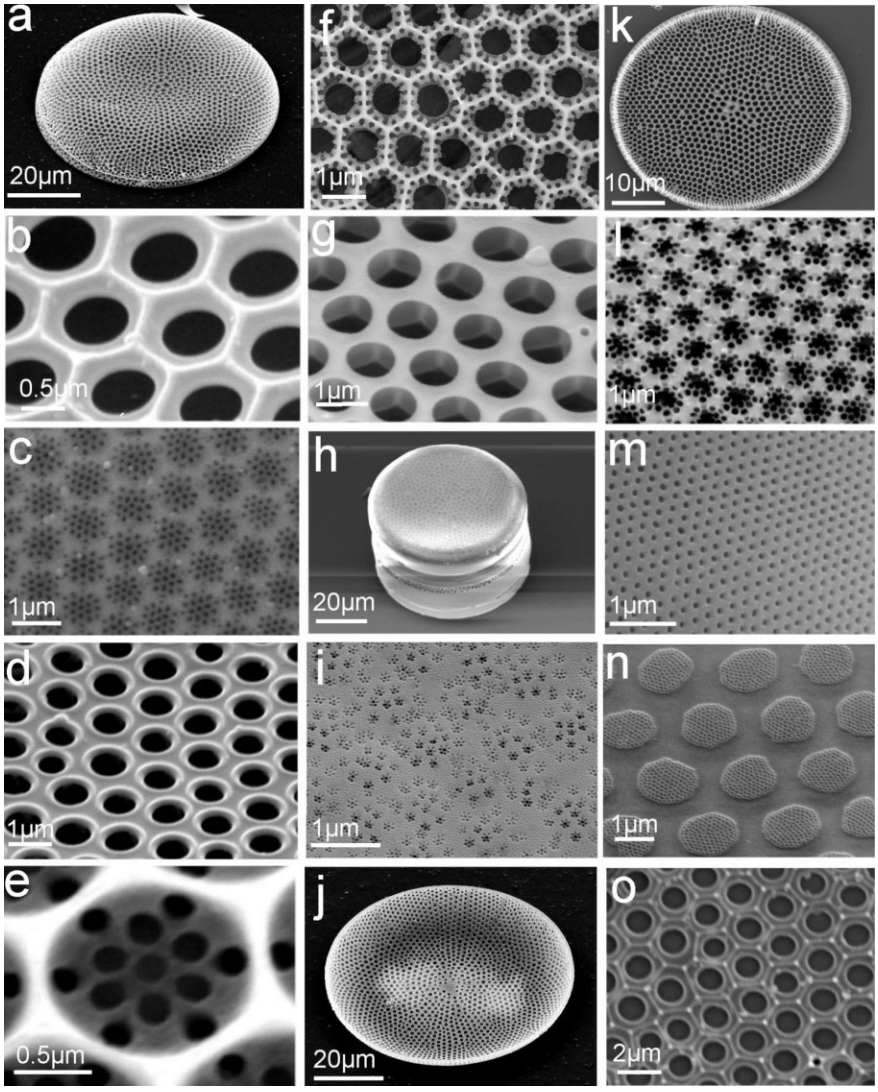

Figure 1. SEM images of silica-based microshells (frustules) and their porous parts obtained from three centric marine diatom species (*Coscinodiscus sp.*(a–f, i, j, l, m, o), *T. eccentrica* (g, k, n) and an unidentified specie (h). a) Whole frustule membrane (external side of the diatom); b) areola structures (internal surface of the diatom) in initial stage of formation; c) cribrum surface (second porous layer); d) areola pores (internal surface) e) cribrum surface (central porous layer) in more detail; f) areola structures (internal membrane surface) in later stage of formation; g) external porous layer; h) whole unidentified diatom species (harvested from Derwent River, Tasmania, and cultured in our lab); i) cribellum surface (external porous layer); j) whole frustule membrane (internal side of diatom); k) whole frustula (internal side of the diatom); l) cribrum surface in later stage of formation; m) girdle band (porous silica band surrounding the diatom and holding the two frustule valves together); n) internal porous layer; o) areola structures in initial stage of formation.

make diatoms promising candidates for nanofabrication, especially in combination with low-cost soft-lithographic approaches.

In our previous work we have demonstrated that diatoms can be used as template for nanofabrication of metal nanostructures.[13,14] Complex gold nanostructures were produced by replication from porous diatom frustules with high precision and nano-scale resolution. The aim of the present work is to extend diatom-based nanofabrication using a soft lithographic approach. A schematic diagram of the fabrication approach using diatoms is outlined in Figure 2. Our results demonstrate the ability to generate multiple copies of diatoms based on a replication process that involves the use of diatom frustules as a master mold and transforming their structure into polymers. Two replication steps in this process are performed: the first is transferring the porous frustule pattern onto an elastic polymer such as PDMS to produce a negative replica, and second transferring the soft PDMS pattern onto a hard photo-curable polymer to obtain a positive replica. Polymers are chosen in this study as replication material to demonstrate the approach but many other solidified structures including gels, precursors to ceramics and carbons, luminescent phosphors, salt and colloids could also be used.[15] The replication process and structures of fabricated polymers were characterized by scanning electron microscopy (SEM) and atomic force microscopy (AFM).

2. Results and Discussion

Figure 2 depicts the procedure for fabrication of micro- and nanoscale patterns of polymers by replica molding using diatoms. The process could be summarized in three steps that includes: immobilization of desired diatoms on surface which are used as biological nanostructured masters (Fig. 2a); the transferring of diatom's porous pattern onto elastomeric PDMS polymer (negative replica) by replica molding (Fig. 2b and c), and converting the PDMS replica into positive replica by second replica molding step using desired polymer such as UV curable polymer (NOA 60) (Fig. 2d and e). Three centric diatom species, *Coscinodiscus sp.*, *Thalassiosira eccentrica* (*T. eccentrica*) and unidentified species (from the Derwent River, Hobart, Tasmania) cultured in our laboratory were used as masters for replication. Each of these diatom species features distinct porous structures that consist of a number of porous layers that differ in their pore patterns among layers and between species.[12g] The frustules can be oriented on a surface in such a way as to expose their external (Fig. 2a, concave) or internal surface (Fig. 2f, convex), which doubles the number of possible replicas. Internal layers can be exposed by acid etching, further increasing the number of possible replica patterns.

Figure 3 shows SEM images of *Coscinodiscus sp.* diatom frustules and their polymer replicas fabricated by the replica

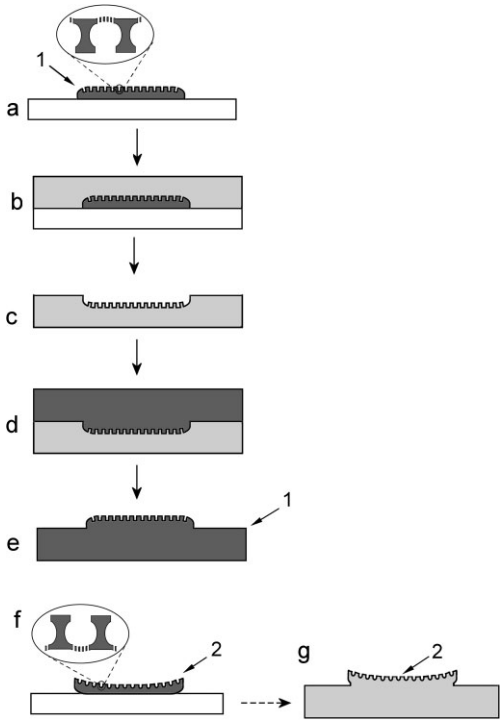

Figure 2. Schematic of the replica molding process using diatom frustules. a) Frustule on surface (concave orientations); b) and c) replication of frustule into PDMS (negative replica) and d) and e) replication of PDMS replica into mercaptol ester type UV curable polymer (NOA 60); f) and g) frustule in convex orientations and their corresponding positive replica.

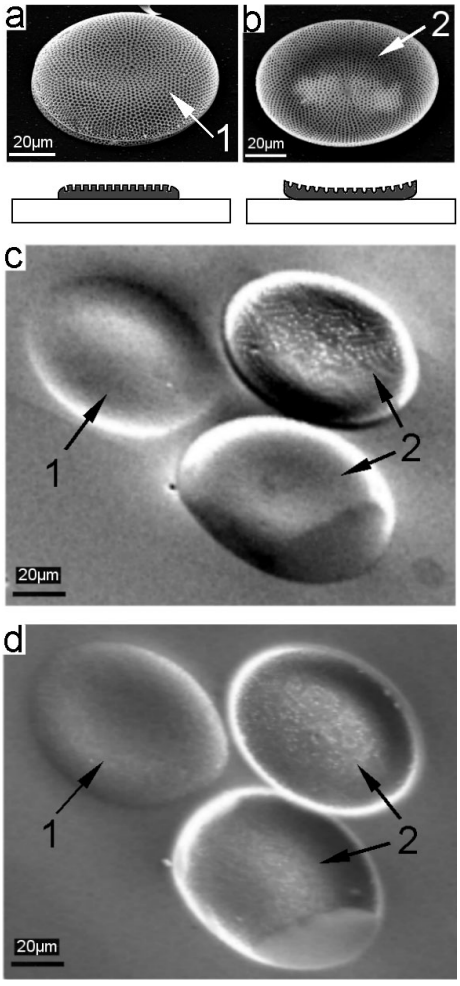

Figure 3. A series of SEM images showing replica molding process of diatom frustule *(Coscinodiscus sp.)* in a) concave orientation (arrow 1) and b) convex orientation (arrow 2) on the substrate surface with c) corresponding PDMS (negative) and d) NOA 60 polymer (positive) replicas.

molding procedure depicted in Figure 2. Similar results were obtained using two other diatom species. First, SEM images (Fig. 3a and b) show diatom frustules in two possible orientations on the surface (concave, Fig. 3a and convex, Fig 3b). Figure 3c presents images of the PDMS replicas (negative) of frustules in both orientations, and Figure 3d their corresponding positive replicas on a mercapto ester photo-curable polymer (NOA 60). The images show that the concave shape from the diatom (Fig. 3a, arrow 1) is transformed into a convex shape of PDMS (Fig. 3c, arrow 1) and then again converted into the initial concave shape in the final positive NOA 60 polymer replica (Fig. 3d, arrow 1). Similar transformation is obtained with initial convex shape of the diatom (Fig. 3b and d, arrows 2). These results confirm that the shape and dimensions of diatoms are successfully transformed into polymer structures in both stages of the replication process. All diatoms immobilized on the surface have been successfully replicated in both replication steps. The method permits the rapid and inexpensive replication of individual diatoms structures.

To demonstrate the precise replication of micro- and nanoscale structures of diatom frustule into polymers, replicas were characterized by SEM and AFM imaging. Figure 4 shows a series of SEM and AFM images of the internal frustule membrane (areola) of *Coscinodiscus sp.* and the corresponding PDMS replica. Images of the whole frustule as well as details of individual pore structures are presented. The main characteristic of the internal frustule layer is the array of radially organized pores (foramen) with an average diameter of about 1200 nm (Fig. 4b and c). At the bottom of the foramen, smaller pores with a diameter of about 190 nm are seen (Fig. 4d). These form part of the external cribrum membrane. The distance between the top of the foramen hole and the cribrum pores as determined by AFM is ~400 nm (Fig. 4d). The corresponding images obtained from the PDMS replica are shown in Figure 4e–h. These images reveal a remarkable level of reproducibility and precision of this replication process. The complex (double) porous structure of diatoms was successfully transferred into a PDMS replica with complex 3D morphology with large cylinder-like structures which are decorated on the top surface by an array of the smaller pillars (Fig. 4f and g). High resolution AFM and SEM imaging confirms that the dimensions of these structures including the height (~400 nm) and diameter (~1200 nm) of the cylinders and the height (~100 nm), and diameter (~200 nm) of smaller pillars (Fig. 4h) are consistent with the dimensions of the foramen and cribrum pores (Fig. 4d). It is evident from the corresponding images

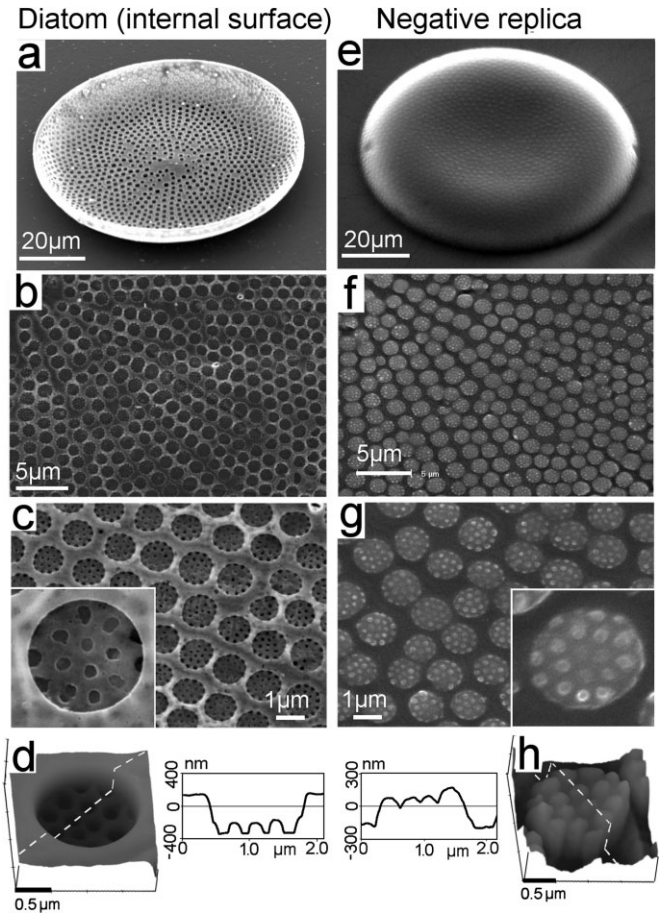

Figure 4. A series of SEM and AFM images (tapping mode) demonstrating the replication of the internal frustule membrane of *Coscinodiscus sp.* a)–c) SEM images of frustule structures used as master showing the organization of porous layers and typical pattern of pores. d) High resolution AFM images with cross-sectional graph presenting an individual foramen perforation with the cribrum membrane at its bottom. e)–g) SEM images of the corresponding PDMS replicas (negative) obtained from frustule showing pattern and shape of replicated porous structures. h) AFM image of the corresponding PDMS structures.

that the observed polymer structures are conformal with the template pores. The quality of the replication of cribrum pores was quite surprising to us because of the small feature size and the curvature of the frustule master, which often impedes PDMS based replica molding to accurately reproduce such small features.

The second replication example is performed using the external frustule membrane of *Coscinodiscus sp.* SEM and AFM images of the frustule used as master and the PDMS replica (negative) fabricated in the first replication step as well as the polymer replica (positive) fabricated in the second replication step are presented in Figure 5. The structure of this frustule layer is best described as a honeycomb of porous domes arranged in a hexagonal pattern (Fig. 5a and b), the domes featuring two kinds of pores: array of smaller pores with a diameter of about 190 nm with 15–20 pores per dome) and larger pores with an irregular shape with a diameter of 400–500 nm arranged in hexagons around the dome perimeter (Fig. 5c).[12g,16] The corresponding PDMS replica fabricated from this frustule layer (Fig. 5d–f) confirms that the frustule shape and porous patterns are successfully reversed in the polymer topography (negative replica). High resolution images (Fig. 5e and f) show that the size and shape of both smaller and larger pillars are in good agreement with pores observed on the frustule master (Fig. 5b and c), again confirming the high precision of the replication process. The negative PDMS replica is then used as a master for further molding into a thermoset polymer mould, but this process could certainly be applied to other materials such as sol-gel ceramics.

The replication of the negative PDMS replica into a positive polymer replica is performed using a photo-curable polymer (NOA 60) and Figure 5g–i shows SEM and AFM images taken from these fabricated polymer replicas. The images demonstrate that frustule shape, porous pattern and porous structures from this second replica are in good agreement with the initial frustule master (Fig. 5a–c). NOA 60 is a suitable material to be employed as a mould for manufacturing soft polymer replicas and could serve as a reusable master for further nanofabrication processes. To reduce adhesion between two polymers (NOA 60 and PDMS) fluorosilane coatings are usually employed. However, our results clearly show that this is not necessary here. NOA 60 could be easily peeled off from PDMS without using fluorosilane agents as surface modifiers, another advantage of using this particular polymer. In our work, we have also explored replica molding from two other diatoms species (*T. eccentrica* and one unidentified species) and successfully fabricated a range of biomimetic polymeric nanostructures (data not shown). We found that the lower size limit of pore replication was about 50 nm. Using hard PDMS, one would expect that even smaller structures could be replicated.

Two different methods of immobilisation of the diatom frustules on the substrate surface were tested (Fig. 2a), immobilization of polylysine coatings and on spin-coated UV curable NOA 60. Diatom frustules immobilized on polylysine coated substrates can only be used once. Some diatoms were removed from the surface or broken during the release of the PDMS layer. In the first case, the removal of diatom remains from PDMS by an additional cleaning procedure, such as ultrasonic cleaning, is required. On the other hand, diatoms immobilized by an ultrathin adhesive NOA 60 film were not removed from the substrate surface and the resulting PDMS replica was free of diatom remains. Therefore, there are no limitations in the number of replications by PDMS and cleaning of PDMS is not necessary. Multiple replications (more than ten times) were performed without morphological defects on diatoms or replicas, which proves that diatom frustules immobilized by this method could be used as reusable masters. A possible disadvantage of this method is that the adhesive could clog underlying pores. To prevent this from happening, the thickness of the NOA 60 spin-coating should not exceed 200 nm.

In this work, we have primarily focused on demonstrating the approach of using diatoms for the rapid replication and fabrication of polymer structures. Our results provide evidence that a variety of biomimetic shapes, geometries and ordered patterns (hexagonal, square) of polymer structures could be

ADVANCED FUNCTIONAL MATERIALS

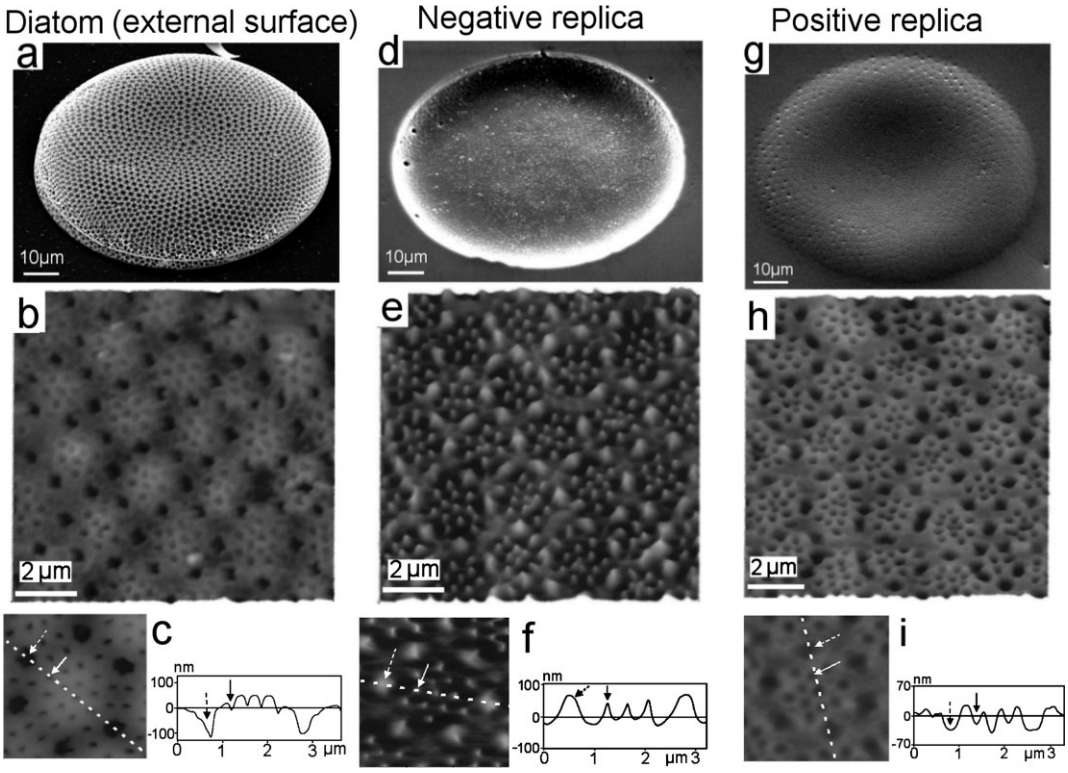

Figure 5. A series of SEM and AFM images (tapping mode) demonstrating replication of the external frustule membrane (cribrum) of *Coscinodiscus sp.* a) SEM and b,c) AFM images of frustule structures used as master showing typical pattern of pores and their shapes. d) SEM and e,f) AFM images of the corresponding PDMS replicas (negative) obtained from the frustule showing pattern and shape of the replicated porous structures. g) SEM and h,i) AFM images of the positive polymer replicas (NOA 60).

fabricated by replica molding from the silica frustules of diatoms. Instead of replica molding, other soft lithographic techniques such as micro contact printing, microtransfer molding and embossing based on diatoms and their replicas could certainly also be applied. It should be emphasized here that the diatom's silica structures, as designed by nature, might have useful optical and in particular photonic properties due to the highly ordered arrangement of features on the submicron scale.[10a,12e] It is therefore reasonable to expect that the fabricated polymer replicas also display interesting properties that might spark further technological applications.

PDMS and NOA 60 are both optically transparent and inexpensive polymers, have valuable mechanical, chemical and optical properties that are compatible with mass replication technologies and are frequently used in applications such as photonics, microfluidics and bioassays. PDMS elastomers for miniaturized bioassays have numerous advantages over silicon and glass: PDMS is easy to fabricate, manipulate and bond to other surfaces, is impermeable to water, non-toxic to cells and permeable to gases and hence very compatible with biological studies. Fabrication of diffractive and optical elements (microlenses, gratings, elastomeric optics, bioinspired micro optics etc.) based on PDMS and soft lithographic approach has been reported.[17] Nano- or microscale two-dimensional arrays generated by soft-lithographic techniques have been used for selective adsorption of proteins, cells, magnetic particles, polystyrene and silica particles, DNA or oligonucleotides-functionalized gold particles etc.[18] Figure 6a presents an example of a positive replica (NOA 60) fabricated from diatom frustule of an unidentified diatom species that was harvested in the Derwent River in Tasmania. The size (diameter 50–80 μm) and shape of the frustule are precisely preserved in the replica. The fabricated diatom replicas with an array of ordered micro- to nanoscale wells (Fig. 6b and c) offer possibilities for use as templates to fabricate structures with higher complexity. We have demonstrated that polystyrene or silica particles can be stored within these nanowells, as shown in AFM images (Fig. 6d and e). It is therefore quite conceivable that polymer replicas could be adapted as chemically addressable platforms for biosensing or microbead-based libraries.

As indicated above, the size of the pores and their highly ordered arrangement are suggestive of interesting optical properties.[19] We therefore opted to study the laser diffraction pattern of the fabricated replicas in the far field (Fig. 7a). As Figure 7b and c demonstrate, we were able to obtain hexagonal diffraction peaks corresponding to zeroth, first and even second order diffraction patterns which demonstrates the high degree of order of the replicated structures and their suitability as biomimetic transmission diffraction gratings. It should be noted that similar diffraction patterns were also obtained from the diatom frustules (data not shown).

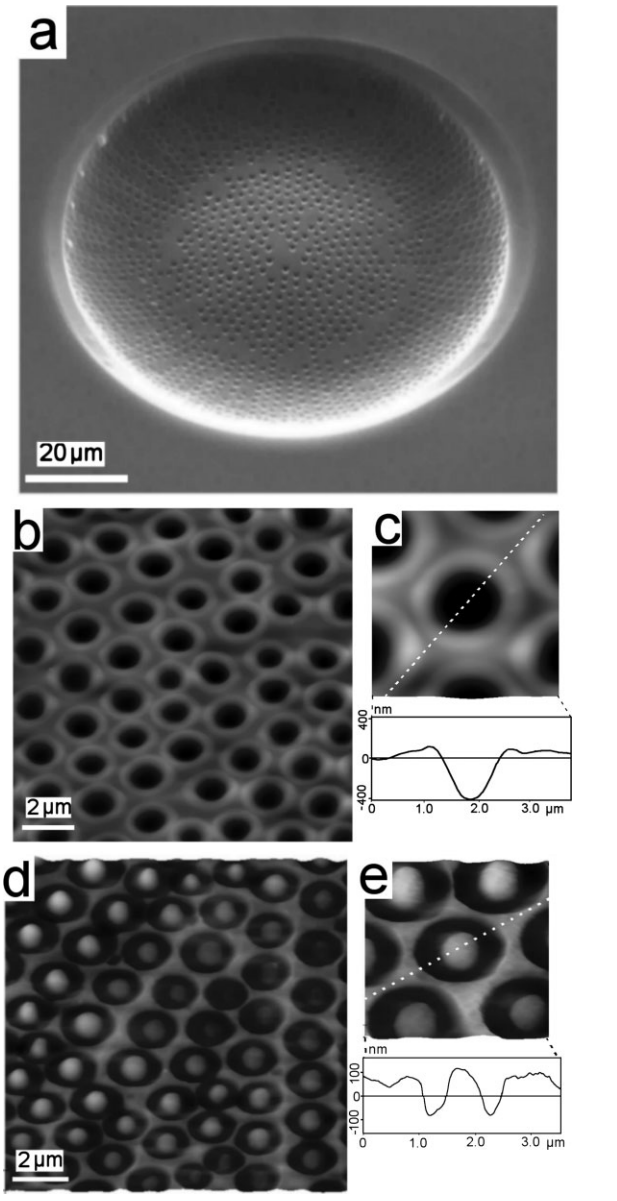

Figure 6. a) SEM image of a positive replica (made of NOA 60) obtained from unidentified diatom specie (from the Derwent River in Tasmania) showing the preservation of diatom frustule shape. b,c) AFM images (contact mode) of positive replica with nanowell-array including graph of single nanowell before deposition of nanoparticles. d,e) AFM images (tapping mode) of polystyrene nanoparticles (490 nm diameter) in nanowells with corresponding cross-section graph.

3. Conclusions

Diatom frustules are biominerals with an enormous number of different structures and patterns with micro- and nanoscale features that offer considerable potential for nanofabrication. This work is the first demonstration that diatom frustules can be replicated into a diverse range of polymer structures with complex and unique morphologies using a replica molding approach. Two polymers (PDMS and NOA 60) were used to fabricate negative and positive replicas from the frustule master.

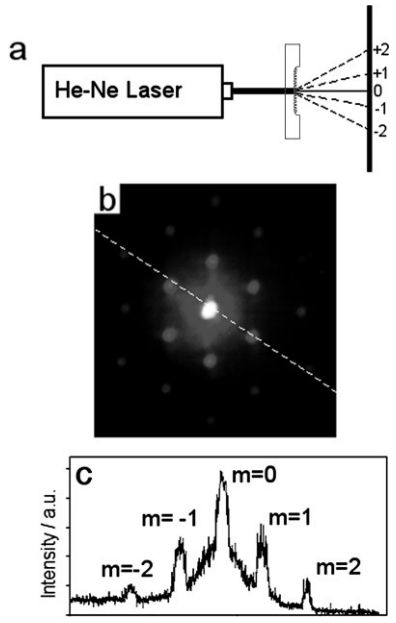

Figure 7. a) Scheme of the experimental set-up used to obtain laser diffraction patterns from the fabricated polymer replicas. b) Image of laser diffraction of negative PDMS replica obtained from *Coscinodiscus sp.* c) Diffraction pattern graph showing up to second order diffraction peaks and a hexagonal diffraction pattern.

Our results attest nanoscale resolution and high precision and reproducibility for this replication process. Polymer replicas were fabricated from three different diatom species demonstrating that this approach not limited to one particular species and pattern. Polymers were chosen in this study as replication material to demonstrate the approach but many other solidified structures including gels, precursors to ceramics and carbons, luminescent phosphors, salts and colloids could also be used. The possible applications for fabricated polymer replicas include optical elements, masters for nanofabrications, biosensing device components and nanoreactors. Laser diffraction in the far field was demonstrated on the diatom replicas and second order diffraction peaks were observed. Lastly, the assembly of polystyrene nanoparticles in the ordered nanowells of the replicas was demonstrated to indicate their potential practical application as chemically addressable platform for biosensing. Diatoms can be routinely grown under laboratory conditions. The key advantage of the described simple and rapid fabrication method therefore is that diatoms are a cheap resource to a tremendous number of masters with a variety of patterns and structures spanning the micro- and nanoscale.

4. Experimental

Chemicals and Materials: Poly(dimethylsiloxane) PDMS, Sylgard 184, was purchased from Dow Corning, USA, mercaptol ester UV curable prepolymer, NOA 60 (Norland Optical adhesives 60) was purchased from Norland Products Inc. (USA). Monodispersed polystyrene (PS) beads (≤490 nm) and aqueous dispersions of monodispersed silica colloids (≤490 nm) were obtained Bangs Laboratories, Inc. (USA).

Polylysine (0.01 %) and EDTA were purchased from Aldrich, Australia.

Culturing of Diatoms: Three centric diatom species; *Coscinodiscus sp.* and *Thalassiosira eccentrica* and one unidentified species (from the Derwent River, Hobart, Tasmania) were obtained from the CSIRO, Marine Division (Hobart, Tasmania, Australia). These cultures were maintained at 20 °C using a 12 hour light/12 hour dark cycle. GSE medium was used to culture *Coscinodiscus sp.* and Guillard's medium (f/2) was used for *T. eccentrica* and the unidentified species [20]. The live diatoms were harvested after 2–3 weeks of culturing and cleaned in sulfuric acid using a procedure described elsewhere [21,22]. This treatment causes the separation of the diatom frustule into the 2 frustule valves and girdle band. Cleaned frustule valves for both procedures were stored in 100 % ethanol.

Replica Molding from Diatoms: Figure 2 summarizes the procedure of replica moulding process using diatoms which includes: immobilization of desired diatom frustule on surface (Fig. 2a); the transferring of diatom's porous pattern onto elastomeric PDMS polymer (negative replica) by replica molding (Fig. 2b and c), and converting the PDMS replica into positive replica by second replica molding step using desired polymer such as UV curable polymer (NOA 60) (Fig. 2d and e).

Two procedures for diatom immobilization on surface were performed. In the first approach, silicon wafer coated with polylysine (from 0.01 % aqueous solution of polylysine) were used. A drop of cleaned frustule suspension was deposited onto cleaned and modified silicon wafer. Frustules settled on the substrate surface exposing either their external surface (concave) or internal surface (convex), which have different porous structures (Fig. 2a). These diatom frustules served as disposable master where the porous structure is replicated into polymer by the moulding process. To employ diatoms as a reusable master, a second immobilisation approach uses an ultra-thin adhesive film of a mercaptol ester UV curable polymer (NOA 60). Owing to its high adhesiveness and transparency, it is generally used as a UV-curable optical adhesive for purposes such as fixing cells or tissue and as a film coating [23]. The ultra-thin adhesive film is prepared by spin-coating onto silicon wafers or glass which allows the strong fixation of frustules on the surface. In average about 50 diatoms randomly orientated and dispersed on surface were immobilised on a spot of 2 mm in diameter using both approaches.

The first replication of diatoms was performed using a replica moulding procedure described elsewhere [4–6]. Briefly, a degassed prepolymer of poly(dimethyl)siloxane (PDMS) was poured carefully over a diatom decorated substrate and cured for at least 6 h at 60 °C (Fig. 2b). After curing, the cross-linked elastomeric PDMS is carefully peeled from the surface and cleaned by sonication and water and ethanol to remove any remains of diatoms. Both surfaces before and after releasing the PDMS were examined by light microscope to confirm the replication process and cleanness of the replicas. PDMS replicas were then used as master for replication into a second polymer using commercial mercaptol ester photo-curable prepolymer (NOA 60).

The prepolymer was poured on the PDMS and cured under UV light ($\lambda = 365$ nm) using a UV lamp as a light source (Fig. 2d). Precuring for 20 min was followed by postcuring for at least 3 h. The polymer mould was then peeled off the PDMS yielding the relief of the initial diatom structure (positive replica) (Fig. 2e). Polystyrene and silica nanoparticles have been assembled in nanowells of positive polymer replica using their aqueous colloidal dispersions adapting the deposition procedure described elsewhere [24].

Instrumentation: The structural characterizations of prepared frustule samples and their corresponding polymer replicas were performed by using scanning electron microscopy (SEM) and atomic force microscopy (AFM).

SEM images were acquired using a Philips XL 30 field-emission scanning electron microscope operating at 2–10 kV. Samples were coated with a thin platinum layer (3–5 nm) and mounted on microscopy stubs with carbon sticky tape.

AFM imaging was performed using a Nanoscope IV Multimode SPM (Veeco Corp., Santa Barbara, USA) using both contact and tapping mode in air using both E scanner (15 μm scan) and J scanner (100 μm scan). Oxide-sharpened silicone nitride probes (NP-S, Veeco Corp. USA) of spring contact $k = 0.15\ \mathrm{N\,m^{-1}}$ were used for contact mode experiments. Silicon probes (NT-MDT, Moscow, Russia) with 150–350 kHz resonance frequencies were used for tapping mode imaging. These probes were cleaned in a water plasma (6 mA source, 0.05 Torr water) for 3 min and characterized using a silicon calibrating grating (TGT 01, Silicon-MDT Ltd., Russia). Different parts of the diatom frustule including external and internal porous layer and their corresponding polymer replicas were characterized. Image processing was performed using Nanoscope off-line software (Veeco Corp.) and SPIP (Image Metrology, Denmark).

Laser Diffraction: The diffraction pattern of the polymer replica (*Coscinodiscus sp.*) transmission grating was obtained in transmission mode using a He-Ne laser with a beam diameter of about 20–30 μm. The resulting diffraction pattern was visualized on a screen in the far field (10–20 cm) from the front of the sample and captured by a CCD camera.

Received: September 22, 2006
Revised: December 13, 2006
Published online: August 7, 2007

[1] M. Geissler, Y. N. Xia, *Adv. Mater.* **2004**, *16*, 12469.
[2] M. J. Madou, *Fundamentals of Microfabrication*, CRC Press, Boca Raton, FL **1997**.
[3] S. Matsui, Y. Ochial, *Nanotechnology* **1996**, *7*, 247.
[4] Y. Xia, G. M. Whitesides, *Angew. Chem. Int. Ed.* **1998**, *37*, 550.
[5] Y. Xia, J. A. Rogers, K. E. Paul, G. M. Whitesides, *Chem. Rev.* **1999**, *99*, 1823.
[6] Y. Xia, G. M. Whitesides, *Annu. Rev. Mater. Sci.* **1998**, *28*, 153.
[7] B. D. Gates, Q. Xu, J. Love, D. B. Wolfe, G. M. Whitesides, *Annu. Rev. Mater. Res.* **2004**, *34*, 339.
[8] a)Y. Xia, J. J. McClelland, R. Gupta, D. Qin, X. M. Zhao, L. L. Sohn, R. J. Celotta, G. M. Whitesides, *Adv. Mater.* **1997**, *9*, 147. b) J. L. Wilbur, E. Kim, Y. N. Xin, G. M. Whitesides, *Adv. Mater.* **1995**, *7*, 649. c) J. C. McDonald, G. M. Whitesides, *Acc. Chem. Res.* **2002**, *35*, 491. d) N. L. Rosi, C. A. Mirkin, *Chem. Rev.* **2005**, *105*, 547.
[9] a) B. Man, G. A. Ozin, *Nature* **1996**, *382*, 313. b) M. Srinivasarao, *Chem. Rev.* **1999**, *99*, 1935. c) M. Sarikaya, C. Tamerler, A. K.-Y. Jen, K. Scholten, F. Baneyx, *Nat. Mater.* **2003**, *2*, 577.
[10] a) M. Sumper, E. Brunner, *Adv. Funct. Mater.* **2006**, *16*, 17. b) F. C. Meldrum, R. Seshadri, *Chem. Commun.* **2000**, 29. c) I. Aizenberg, *Adv. Mater.* **2004**, *16*, 1295. d) E. Dujardin, S. Man, *Adv. Eng. Mater.* **2002**, *4*, 461.
[11] F. E. Round, R. M. Craford, D. G. Man, *The Diatoms*, Cambridge University Press, Cambridge **1990**.
[12] a) J. Parkinson, R. Gordon, *Trends Biotechnol.* **1999**, *17*, 190. b) E. G. Vrieling, T. P. M. Beelen, R. A. van Santen, W. W. C .Gieskes, *J. Biotechnol.* **1999**, *70*, 39. c) R. W. Drum, R. Gordon, *Trends Biotechnol.* **2003**, *21*, 325. d) N. L. Rosi, C. S. Thaxton, C. A. Mirkin, *Angew. Chem.* **2004**, *116*, 5616. e) T. Fuhrmann, S. Landwehr, M. E. Rharbi-Kucki, M. Sumper, *Appl. Phys. B* **2004**, *78*, 257. f) C. E. Hamm, *J. Nanosci. Nanotechnol.* **2005**, *5*, 108. g) D. Losic, G. Rosengarten, J. G. Mitchell, N. H. Voelcker, *J. Nanosci. Nanotechnol.* **2005**, *6*, 982. h) D. Losic, G. Triani, P. J. Evans, A. Atanacio, J. G. Mitcheli, N. H. Voelcker, *J. Mater. Chem.* **2006**, *16*, 4029.
[13] D. Losic, J. G. Mitchell, N. H. Voelcker, *Chem. Commun.* **2005**, 4905.
[14] D. Losic, J. G. Mitchell, N. H. Voelcker, *New J. Chem.* **2006**, *30*, 908.
[15] C. A. Mirkin, J. A. Rogers, *MRS Bull.* **2001**, *26*, 506.
[16] D. Losic, R. J. Pilar, T. Dilger, J. G. Mitchell, N. H. Voelcker, *J. Porous Mater.* **2007**, *14*, 61.
[17] a) J. L. Wilbur, R. J. Jackman, G. M. Whitesides, *Chem. Mater.* **1996**, *8*, 1380. b) C.-Y. Chang, S.-Y. Yang, L.-S. Huang, T.-M. Jeng, *J. Micromech. Microeng.* **2006**, *16*, 999.

[18] a) D. G. Anderson, S. Levenberg, R. Langer, *Nat. Biotechnol.* **2004**, *22*, 863. b) K.-B. Lee, S.-J. Park, C. A. Mirkin, J. C. Smith, M. Mrksich, *Science* **2002**, *295*, 1702. c) Y. Yin, Y. Lu, B. Gates, Y. Xia, *J. Am. Chem. Soc.* **2001**, *123*, 8718.

[19] a) M. V. Kunnavakkam, F. M. Houlihan, M. Schlax, J. A. Lidle, P. Kolodner, O. Nalamasu, J. A. Rogers, *Appl. Phys. Lett.* **2003**, *82*, 1152. b) M.-H. Wu, G. M. Whitesides, *Adv. Mater.* **2002**, *14*, 1502.

[20] R. R. L. Guillard, J. H. Ryther, *Can. J. Microbiol.* **1962**, *8*, 229.

[21] G. R. Hasle, G. A. Fryxell, *Trans. Am. Micros. Soc.* **1970**, *89*, 469.

[22] M. S. Hale, J. G. Mitchell, *Aquat. Microb. Ecol.* **2001**, *24*, 287.

[23] a) O. Cazarola, A. Lacampagne, J. Fauconnier, G. Vassort, *Br. J. Pharmacol.* **2003**, *139*, 99. b) S. Zauscher, D. J. Klingenberg, *J. Colloid Interface Sci.* **2000**, *229*, 497.

[24] M. Kang, S. Yu, N. Li, C. R. Martin, *Langmuir* **2005**, *21*, 8429.